Int. J. Heat Mass Transfer. Vol. 36, No. 17, pp. 4207–4213, 1993
Printed in Great Britain

0017–9310/93 $6.00 + 0.00

Forced convective heat transfer in a vertical annulus filled with porous media

BU-XUAN WANG and JIAN-HUA DU
Thermal Engineering Department, Tsinghua University, Beijing 100084, China

(*Received* 8 *May* 1993)

Abstract—Experiments on forced convective heat transfer were conducted for water or transformer-oil flowing upward through a vertical annulus filled with different size porous media. The thermal dispersion caused by successive flow disturbance due to the existence of porous media may have significant influence on the *Nu* value in the thermally fully-developed region, and a new model is proposed to consider the thermal dispersion as related to the geometrical parameters of porous media and the flow characteristics. The temperature distribution near the wall surface, and hence the convective heat transfer coefficient, can be thus predicted, which agrees well with the experimental results.

1. INTRODUCTION

THE CONVECTIVE heat transfer in a porous medium has been the subject of intensive studies in recent years, because of its important practical application in such fields as agriculture, chemical engineering, geothermal and petroleum reservoir engineering, environmental protection, material science, thermal insulations, grain and coal storage, underground water hydrology, soil mechanics, drying technology, transpiration cooling, solid matrix heat exchanger, and processing of foods, etc. Consequently, the fundamental understanding for these associated heat and mass transport processes is of critical importance.

The overwhelming majority of existing studies are pertinent to fluid flow and heat transfer in porous media based on the Darcy flow model [1]. The theoretical works of Vafai and Tien [2] attempted to account for boundary and inertial effects on forced convective flow in porous media. Vafai [3] and Vafai *et al.* [4] studied the effects of flow channeling on forced convection along a flat plate theoretically and experimentally. Kaviany [5] investigated a laminar flow through a porous medium bounded by isothermal parallel plates with the Brinkman-extended flow model and constant matrix porosity. Poulikakos and Renken [6] analyzed theoretically the forced convection in a channel filled with porous medium, and accounted for the effects of flow inertia, variable porosity, and Brinkman friction. Cheng and Hsu [7] inspected the wall effect on the thermal dispersion process for forced convective flow through an annular packed sphere-bed. Cheng and Zhu [8] studied the effects of radial thermal dispersion on fully-developed forced convection in cylindrical packed tubes. Kuo and Tien [9] introduced the mixing-length concept and statistical averaging method to depict the transverse dispersion process in packed sphere-beds. Hsu and Cheng [10] reviewed their studies on the thermal dispersion in porous medium and derived the thermal dispersion conductivity tensor for convection based on the volume averaging of the velocity and temperature deviations in the pores.

To the authors' knowledge, only a few experimental investigations have been reported on forced convection in a packed channel. Verschoor and Schuit [11] conducted their experiments on forced convection of air in a cylindrical packed tubes with uniform surface temperature, while Quinton and Storrow [12] performed experiments on a similar geometry but with uniform wall heat flux. Yagi and Kunii [13] carried out experiments for forced convection of air in an annular packed tube comprised of glass beads heated asymmetrically. The experiments of Schroeder *et al.* [14] focused on convection of water in a packed bed between parallel plates heated asymmetrically. All these mentioned experiments were limited to the fully thermal-developed region. More experimental and theoretical studies on convective heat transfer in the porous medium are still needed for better understanding of the transport processes in porous media. In this paper, experiments for flow and convective heat transfer of water or transformer-oil in a concentric annuli filled with different size glass beads have been conducted, and analyzed theoretically with emphasis on the thermal dispersion in porous media.

2. EXPERIMENTAL STUDY

Figure 1 shows the schematic diagram of the experimental system set up. It is composed of constant-temperature reservoir, pump, experimental section, cooler and measurement apparatus. The reservoir has volume of 0.1 m^3; the cooling coil inserted in the reservoir is provided to control and keep the constant fluid temperature the same as that at the entrance of the experimental section. The pump keeps fluid

NOMENCLATURE

A_m	amplitude of the oscillation of porosity nearby the wall
a	empirical constant in equation (9)
b	empirical constant in equation (9)
C_t	empirical constant in the thermal dispersion conductivity
D_e	equivalent diameter of channel [m]
d_p	diameter of packed beads [m]
f	weighted coefficient in equation (13)
H	width of channel [m]
h_w	heat transfer coefficient [W m^{-2}]
K_d	stagnant conductivity [W m^{-1} °C^{-1}]
K_e	effective conductivity [W m^{-1} °C^{-1}]
K_f	conductivity of fluid [W m^{-1} °C^{-1}]
K_t	thermal dispersion conductivity [W m^{-1} °C^{-1}]
l	dimensionless mixing length in equation (4)
Nu	Nusselt number
Pe	Peclet number
Pr	Prandtl number
q_w^*	heat flux on the heating surface [W m^{-2}]
Re_p	Reynolds number based on the packed beads
T	temperature [°C]
y	distance from the wall surface [m].

Greek symbols

γ	coefficient in equation (6)
φ	porosity
ω	empirical coefficient in equation (5).

Subscripts

f	quantity associated with the fluid
p	quantity associated with packed beads
t	quantity associated with thermal dispersion
w	quantity associated with wall
x	local quantity.

Superscript

*	dimensionless quantity.

circulating in the system; the valves regulate the flow and the direction of fluid.

Figure 2 shows the structure of the experimental section in detail. A concentric annular passage consisted of a stainless inner tube of 9.5 mm O.D. and a stainless outer tube of 28 mm I.D. and 790 mm long. Two stainless-steel nets with screens made of insulating material are placed at the inlet and outlet of the passage, respectively, to hold the porous material in place. The packed bed with glass beads of ϕ0.7 mm and ϕ2.5 mm are chosen as the porous medium. Special care has been taken in packing the glass beads to ensure uniformity of the porous medium. The passage was randomly packed by the bead particles settled in water after stirring and then tamped down slightly, levelled and shocked to fill about 2 cm until no more beads could be packed into the channel. The experimental section was heated by alterating current passing through the inner tube directly to form a boundary condition of uniform heat flux, while the outer tube

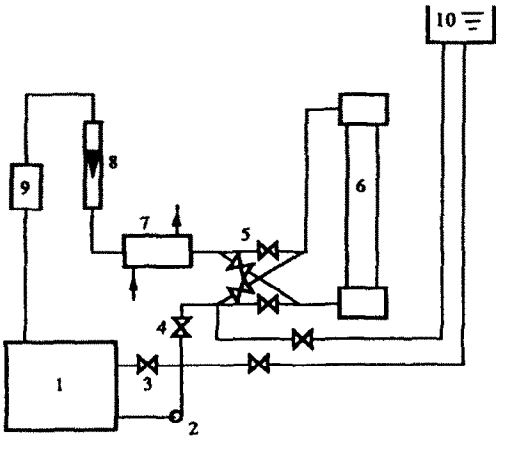

FIG. 1. Schematic diagram of the experimental system: (1) reservoir, (2) pump, (3), (4), (5) valves, (6) experimental section, (7) cooling coil, (8) rotameter, (9) flow measurement apparatus, (10) high level tank.

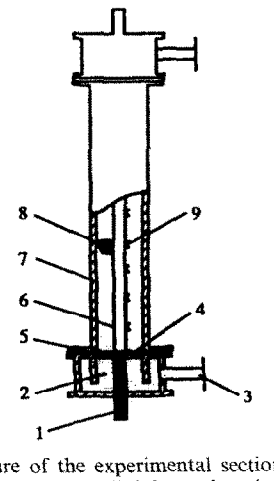

FIG. 2. Structure of the experimental section: (1) heating polar, (2) mixing rooms, (3) inlet and outlet of the experimental section, (4) connecting flange, (5) stainless-steel nets, (6) heating tube, (7) outer tube, (8) packed beads, (9) thermocouples.

was insulated. Twenty-nine copper–constantan thermocouples were arranged along the inner tube surface to measure the axial temperature distribution along the heating surface. All the thermocouples inserted were calibrated with overall accuracy within $\pm 0.1°C$. The maximum surface temperature of the heating surface was limited to 95°C to prevent the occurrence of boiling.

Prior to testing, air bubbles were eliminated by degassing the experimental system by heating and vibrating repeatedly to ensure that the experimental section is in a liquid-saturated state. The test generally proceeded by maintaining the required flow rate, input power and inlet fluid temperature. The steady state was assumed to be established if the wall temperature and local bulk fluid temperatures changed within 0.15°C during 10 min. Then the data of flow rate from rotameter, inlet fluid temperature, the temperature distribution on the heating surface, the electric power input and the bulk temperature at the outlet of the experimental section were recorded. The heat balance was found to be less than 5%. The local heat transfer coefficient h_x was calculated by the local heat flux, the local wall temperature and the local bulk mean fluid temperature. The Nusselt number based on the particle diameter, Nu_x, was evaluated as:

$$Nu_x = h_x d_p / k_f = q''_w d_p / [k_f (T_{wx} - T_{bx})] \quad (1)$$

where q''_w is the heat flux on the heating surface, T_{wx} and T_{bx} are the local wall temperature and bulk mean fluid temperature, respectively. All of the fluid properties were taken at the local mean film temperature, i.e. the arithmetic mean of the corresponding local bulk fluid temperature and local wall temperature.

Figure 3 illustrates the variation of Nusselt number for water flowing along the thermal entry region for a range of flow rate from 5 to 15.2 g s^{-1}, with the passage filled with $\phi 0.7$ mm glass beads. The experimental results show that, the development of thermal boundary in the packed concentric annuli is faster than that in the empty concentric annuli, but it is not as fast as the development of velocity boundary layer. The higher the flow rate, the longer the thermal entrance length. When $(x/D_e) > 30$, the thermal boundary can be considered as fully-developed. The Nusselt number for the thermally-developed region changes with Re_p, and hence is quite different from that for the laminar flow through empty annuli, for which Nu depends only upon the wall thermal conditions. This is due to the lateral mixing of fluid due to 'turbulence' caused by successive flow disturbance through packed beds, i.e. the significant effect of thermal dispersion on the thermal boundary layer development and therefore on the heat transfer coefficient.

Figure 4 shows the experimental results for water flowing through the passage filled with $\phi 2.5$ mm glass beads. Compared with Fig. 3, it is easy to find that, owing to the channelling effect, the development of thermal boundary layer for the smaller beads packing is faster than that for the larger beads packing.

3. MODELING OF THE THERMAL DISPERSION AND WALL FUNCTION

Dispersion is one of the main characteristics of transport phenomena in porous medium. The effect of dispersion is similar to that of turbulence, but turbulence is developed from the instability of fluid flow, while dispersion is caused by successive flow disturbances though a porous medium which forces the flow to undergo a tortuous path around the solid beads. Dispersion effects become dominant for the case of high Peclet number, and may play a reasonably significant role for the cases of low Peclet number.

As shown by the above-mentioned experimental results, the thermal dispersion has significant effect on the thermal boundary-layer development, and hence on the convective heat transfer in packed beds. Kwong and Smith [15] developed first the concept of 'effective conductivity', K_e by considering the heat diffusion of fluid coupled with the thermal dispersion in a porous medium. It is the sum of stagnant conductivity K_d and the thermal-dispersion conductivity K_t when fluid flows through the porous medium, i.e.

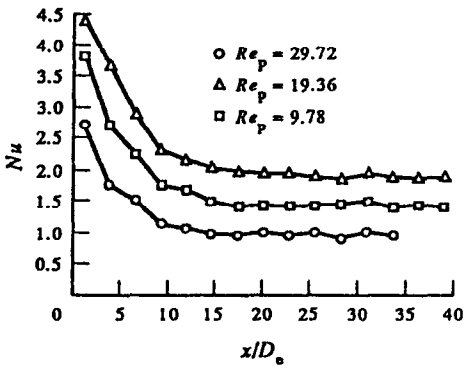

FIG. 3. Nu_x vs x/H for water when $H/d_p = 13.21$: (1) $m = 15.2$ g s^{-1}, (2) $m = 9.9$ g s^{-1}, (3) $m = 5.0$ g s^{-1}.

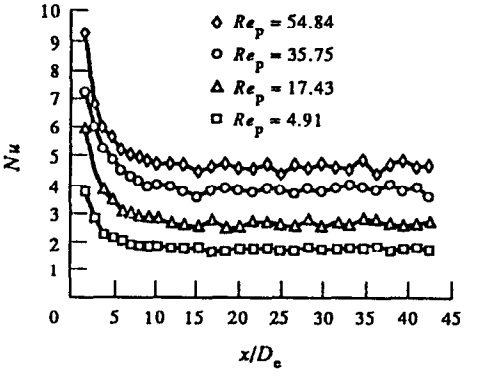

FIG. 4. Nu_x vs x/H for water when $H/d_p = 3.7$.

$$K_e = K_d + K_t \tag{2}$$

where K_d can be evaluated by the formula proposed by Zehener [16] and K_t evaluated by the following empirical relation:

$$K_t/K_f = C_t Re_p Pr_f. \tag{3}$$

Here Re_p is the Reynolds number based on the diameter of the packing beads of the porous medium, Pr_f is Prandtl number of the fluid, and C_t is an empirical constant determined by experiments.

From previous experiments reported in refs. [13, 14], it has been observed that steep radial temperature gradients exist near the heated or cooled wall in the packed channel. The variation of porosity near the wall affects the stagnant conductivity, and the wall causes the reduction of lateral mixing of fluid. As a result, the thermal dispersion conductivity reduces. This is so called the 'channeling effect'.

Cheng and Hsu [7] have analyzed the phenomena of steep temperature gradients in forced convection in a packed channel by taking into consideration the effects of thermal dispersion, variable porosity, and nonuniform velocity distribution. They assumed that the local transverse thermal dispersion conductivity K_t is

$$K_t/K_f = C_t Re_p Pr_f l \tag{4}$$

with l being a dimensionless mixing length, normalized with respect to d_p, which can be expressed by a two-layer model in early work and modelled as the Van Driest wall function recently [8],

$$l = 1 - \exp[-y/\omega d_p] \tag{5}$$

with ω introduced as an empirical constant. The empirical constants C_t in equation (4) and ω in equation (5) were obtained by comparing the predicted heat transfer characteristics with experimental data. It depends also upon the empirical values in the porosity distribution equation. Figure 5 shows the comparison of calculation by the above-mentioned model with $C_t = 0.12$, $\omega = 1.0$ and the experimental result of Schroeder *et al.* [14].

Kuo and Tien [9] proposed also a transverse thermal dispersion model similar to equation (4):

$$K_t/K_f = \gamma Re_p Pr_f \tag{6}$$

with the value of γ reduced in both the core and the near wall region. Figure 6 shows the comparison of the theoretical prediction by Kuo and Tien's model and Schroeder's experimental data [14].

We can see from Figs. 5 and 6 that all these thermal dispersion models cannot predict the temperature distribution in the near-wall region, especially when Re_p is small. The region of nonlinear steep temperature distribution is wider than predicted.

Koch and Brady [17] adopted the assemble averaging method to derive the dispersion coefficient. Their results indicate that this coefficient is not a constant, but rather a function of porosity. They also

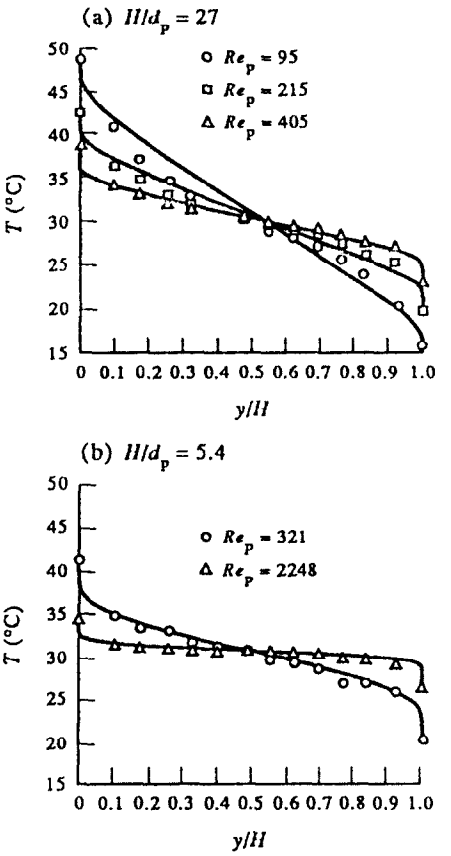

FIG. 5. Prediction of temperature distribution by Cheng's model and Schroeder's data.

showed that the thermal dispersion coefficient would include the mechanical thermal dispersion, which results from the stochastic velocity fluctuation induced in the fluid due to random distributed beads, and the hold-up thermal dispersion in the region of no-slip boundary or zero velocity region, and the thermal dispersion coefficient will be proportional to velocity, u, for irregular packed beds and proportional to $u^{0.1}$ for regular packed beds, i.e.

$$K_t/K_f = C_t' Re_p Pr_f, \quad \text{for randomly packed beds:} \tag{7}$$

$$K_t/K_f = C_t'' Re_p^{0.1} Pr_f, \quad \text{for regular packed beds.} \tag{8}$$

We try to consider the thermal dispersion and wall function together by a weighted combination of the two thermal dispersion expressions and this weighted coefficient should relate to the regularity of the packed beads. It is a well-known fact that the arrangement of beads in the near wall region is restricted by the wall. The first layer of beads contacting the wall could be relatively regular, from the second layer of beads and so on, the arrangement of beads becomes gradually

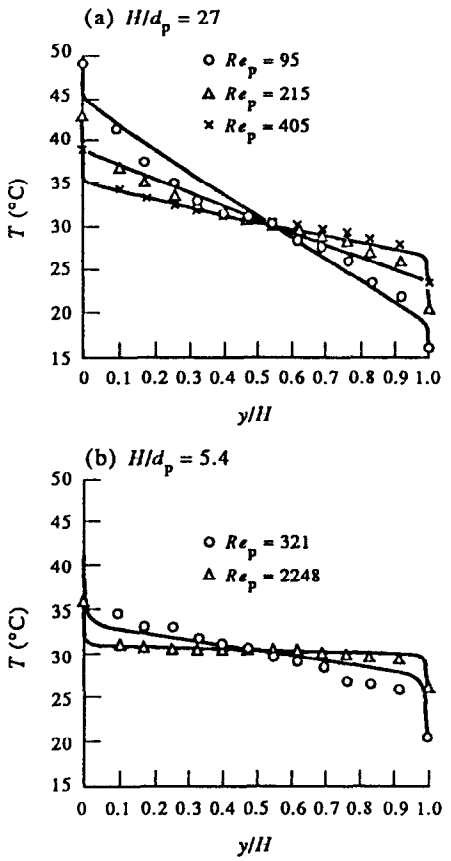

FIG. 6. Prediction of temperature distribution by Kuo's model with Schroeder's data.

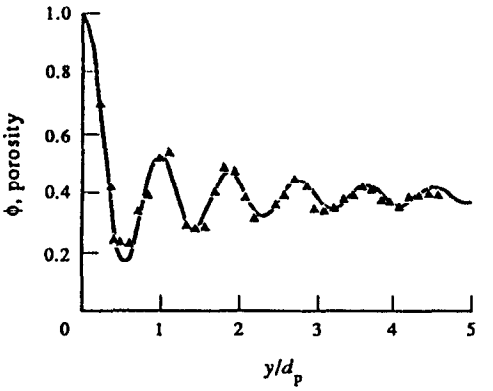

FIG. 7. Prediction of porosity variation by Mueller's model with Benenati's data.

more and more random. The experimental results conducted by Benenati and Brosilow [18] indicated that the variation of porosity near the wall region is in the form of attenuated oscillation which may disappear 4–5 bead diameters from the wall. This variation of the porosity would naturally effect the heat and mass transport in the porous medium. The attenuated oscillation of porosity relates to the regularity of the packed beads. Mueller [19] proposed the variation function of porosity near the wall surface when $(D_c/d_p) > 2.6$ as:

$$\varphi = \varphi_\infty + (1-\varphi_\infty)J_0(ay^*)\exp(-by^*) \quad (9)$$

$$a = 8.243 - 12.98/(H/d_p + 3.156)$$

$$\text{for } 2.61 < H/d_p < 13.0 \quad (10a)$$

$$a = 7.383 - 2.932/(H/d_p - 9.864)$$

$$\text{for } H/d_p \geqslant 13.0 \quad (10b)$$

$$b = 0.304 - 0.724/(H/d_p) \quad (11)$$

$$\varphi_\infty = 0.379 + 0.078/(H/d_p) \quad (12)$$

where $(1-\varphi_\infty)\exp(-by^*)$ is the attenuation factor, which decreases away from the wall surface. The Bessel function $J_0(ay^*)$ characterizes the attenuated oscillation. Figure 7 shows the comparison of the prediction with Mueller's model and Benenati's experimental result for variation of porosity in the near wall region.

The regularity of packed beads could be measured by the amplitude A_m of the oscillation of porosity

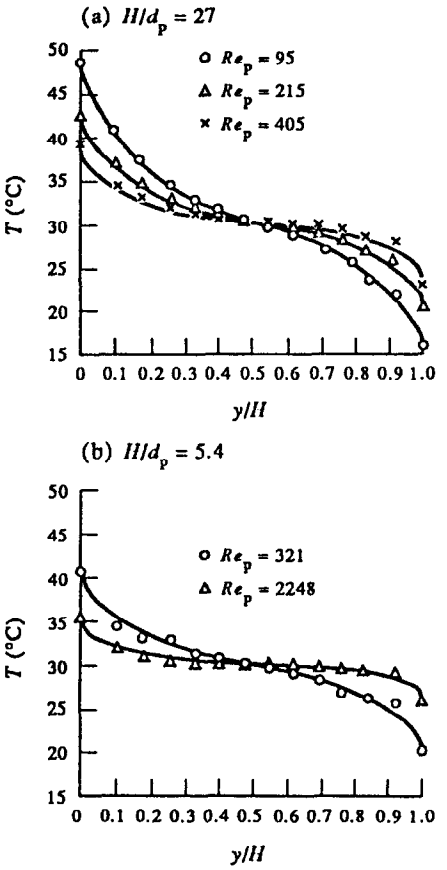

FIG. 8. The prediction of temperature distribution by this model with Schroeder's data.

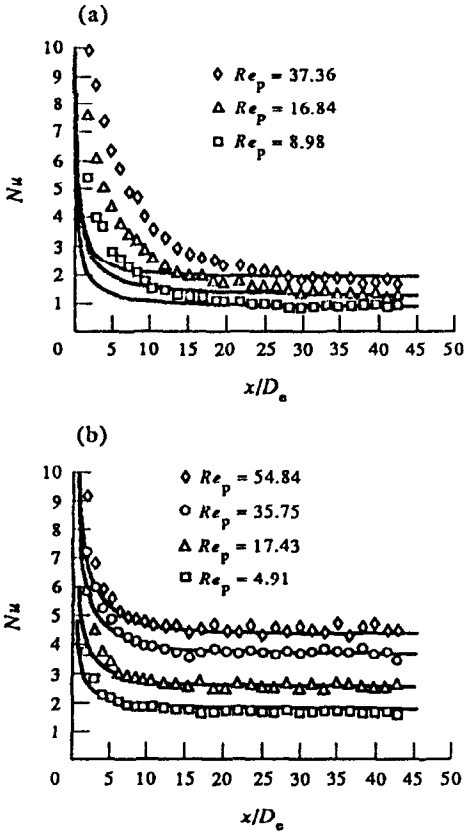

FIG. 9. Prediction of Nu by this model with experimental results for water. (a) Nu_x vs x/H for $H/d_p = 13.21$, (b) Nu_x vs x/H for $H/d_p = 3.7$.

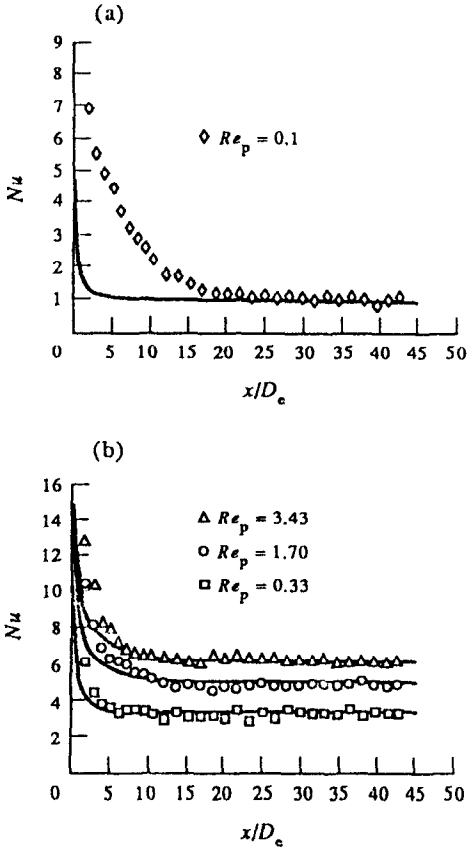

FIG. 10. Prediction of Nu by this model with experimental results for transformer-oil. (a) Nu_x vs x/H for $H/d_p = 13.21$, (b) Nu_x vs x/H for $H/d_p = 3.7$.

near to the wall, and we propose to use the weighted coefficient to describe the thermal dispersion model. For the effects of two walls of a concentric annular channel, the thermal dispersion may be expressed as,

$$K_t/K_f = C_t(1-\varphi)[f\,Pe^{0.1} + (1-f)\,Pe] \quad (13)$$

$$f = \mathrm{Max}\,[A_{m1}(1-A_{m2}), (1-A_{m1})A_{m2}] \quad (14)$$

where, A_{m1}, A_{m2} are the amplitude of oscillation for the porosity nearby the wall 1 and 2 respectively. C_t can be obtained by comparing the predicted distribution of temperature and the experimental data, and in this paper, we take $C_t = 0.1$.

4. THE COMPARISON OF THE PREDICTED AND EXPERIMENTAL RESULTS WITH DISCUSSIONS

Figure 8 shows the prediction of temperature distribution by our model with the data reported by Schroeder *et al.* [14]. It can be seen that this prediction is successful for the actual temperature distribution nearby the wall surface, especially for the low Re_p cases.

Figures 9(a) and (b) and Figs. 10(a) and (b) show the predictions of the convective heat transfer coefficient with the experimental results for water and for transformer-oil, respectively. The predicted results and the corresponding experimental data coincide to each other in the thermal fully-developed region. Some deviations exist in the thermal entrance region. This may come from ignoring the axial thermal dispersion and the variation of transverse thermal dispersion along the flow direction. Comparing Figs. 9 and 10 such deviations for case $H/d_p = 3.7$ are smaller than that for $H/d_p = 13.21$, this may illustrate the difference in channelling effects on the thermal dispersion and on the variations of the thermal dispersion along the flow direction for the core region and near wall region. This needs to be further investigated.

5. CONCLUDING REMARKS

The thermal dispersion caused by the successive flow disturbance significantly affects both the thermal boundary-layer development and the Nu values in the thermally fully-developed region. The thermal dispersion model proposed, which is related to the geo-

metrical parameters of packed beds and the flow characteristics, can predict the actual temperature distribution near the wall surface and hence the convective heat transfer coefficient in thermally fully-developed region. Further experimental and analytical investigations are still needed.

Acknowledgement—The project is financially supported by the Fund from China National Science Foundation (Beijing) with contract No. 59136060.

REFERENCES

1. J. Bear, *Dynamics of Fluid in Porous Media.* Elsevier, New York (1972).
2. K. Vafai and C. T. Tien, Boundary and inertia effects of flow and heat transfer in porous media, *Int. J. Heat Mass Transfer* **24,** 195–204 (1981).
3. K. Vafai, Convective flow and heat transfer in variable porosity media, *J. Fluid Mech.* **147,** 233–259 (1984).
4. K. Vafai, R. L. Alkire and C. T. Tien, An experimental investigation of heat transfer in variable porosity media, *ASME J. Heat Transfer* **107,** 642–747 (1985).
5. M. Kaviany, Laminar flow through a porous channel bounded by parallel plates, *Int. J. Heat Mass Transfer* **28,** 855–858 (1988).
6. D. Poulikakos and K. J. Renken, Forced convection in a channel filled with porous medium, including the effects of flow inertia, variable porosity, and Brinkman friction, *J. Heat Transfer* **109,** 880–888 (1987).
7. P. Cheng and C. T. Hsu, Fully-developed forced convective flow through an annular packed-sphere bed with wall effects, *Int. J. Heat Mass Transfer* **29,** 1843–1853 (1986).
8. P. Cheng and H. Zhu, Effects of radial thermal dispersion on fully-developed forced convection in cylindrical packed tubes, *Int. J. Heat Mass Transfer* **30,** 2373–2383 (1987).
9. S. M. Kuo and C. T. Tien, Transverse dispersion in packed-sphere beds, *The 25th National Heat Transfer Conf.*, Houston, Texas (1988).
10. C. T. Hsu and P. Cheng, Thermal dispersion in a porous media, *Int. J. Heat Mass Transfer* **33,** 1587–1597 (1990).
11. H. Verschoor and G. C. A. Schuit, Heat transfer to fluid flowing through beds of granular solids, *Appl. Sci. Res.* **A2,** 97–119 (1952).
12. J. H. Quinton and A. J. Storrow, Heat transfer to air flowing through packed tubes, *Chem. Engng Sci.* **5,** 245–257 (1956).
13. S. Yagi and D. Kunii, Studies of heat transfer near wall surface in packed beds, *A.I.Ch.E. Jl* **6,** 97–104 (1960).
14. K. J. Schroeder, U. Renz and K. Elegeta, Forschungsberichte des Landes Nordrhein-Westfalen No. 3037 (1981).
15. S. S. Kwong and J. M. Smith, Radial heat transfer in packed beds, *Ind. Engng Chem.* **49,** 894–903 (1957).
16. P. Zehener, Waermeleitfahigkeit won Schuettung be Massigen Temperaturea, *Chemie-Ingr.-Tech.* **42,** 933–941 (1970).
17. D. L. Koch and J. F. Brady, Dispersion in fixed beds, *J. Fluid Mech.* **154,** 321–349 (1985).
18. R. F. Benenati and C. B. Brosilow, Void fraction distribution in beds of sphere, *A.I.Ch.E. Jl* **8,** 359–361 (1962).
19. G. E. Mueller, Prediction of radial porosity distribution in randomly packed fixed beds of uniformly sized spheres in cylindrical containers, *Chem. Engng Sci.* **46,** 706–708 (1991).